Massive oxidation of phospholipid membranes leads to pore creation and bilayer disintegration

Lukasz Cwiklik * and Pavel Jungwirth

Institute of Organic Chemistry and Biochemistry, Academy of Sciences of the Czech Republic and Center for Biomolecules and Complex Molecular Systems, Flamingovo nam. 2, 16610 Prague 6, Czech Republic

Abstract

Oxidation processes in membranes accompany various pathological conditions in organisms, nevertheless the influence of oxidation on the membrane structure is still poorly understood. Here we monitored the time evolution of a massively oxidized dioleoylphosphatidylcholine membrane in molecular dynamics simulations. Oxidation destabilized the membrane and, depending on its extent and type, in some cases even destroyed its structure. Creation of stable pores was observed as a direct consequence of oxidation and we describe here the molecular mechanisms of their formation.

* Corresponding author.
Email address: lukasz.cwiklik@uochb.cas.cz (Lukasz Cwiklik).

Oxidized membrane phospholipids are involved in various pathological conditions including inflammation, atherosclerosis, cancer, type 2 diabetes, and Alzheimer's disease [1–3]. Currently, a coherent overall view of the causalities is still lacking due to insufficient understanding of the cellular and molecular mechanisms. The process of oxidation of the unsaturated acyl chains of the phospholipids introduces polar moieties to the originally hydrophobic parts of lipids, which changes dramatically their biophysical parameters and, consequently, the properties of membranes containing them. In order to unravel the mechanisms of action of oxidized phospholipids in cells it is imperative to obtain a molecular view of the effects of oxidation [4]. Recently, two pioneering Molecular Dynamics (MD) simulations of bilayers containing various amounts of oxidized phospholipids unraveled changes in chain orientations and increase in area per headgroup [5,6]. These observation also point to potential mechanisms of cell damage. However, due to limited degree of oxidation and finite length of the calculations disintegration of the membrane has not been directly simulated yet. It is the purpose of the present MD study to capture with atomistic detail creation of pores and consequent complete destruction of the bilayer induced by massive oxidation of the phospholipids.

In our simulations we started with an intact bilayer of dioleoylphosphatidylcholine (DOPC) in water. We then oxidized one or both of the unsaturated acyl chains of each DOPC molecule and followed the structural changes in the system. By such massive oxidation we managed to destabilize and in some cases even to destroy the bilayer structure at the computationally accessible 0–100 ns timescale. We were also able investigate the influence of the degree and chemical type of oxidation on the stability of the membrane. As observed experimentally, in phospholipid membranes there are several possible oxidation

Table 1

Composition of oxidized bilayers. Terminal groups at cleavage sites of chains are specified.

system	sn-1	sn-2	short-chains
OX1	-CHO	non-oxidized	-CHO
OX2	-CHO	non-oxidized	$-CH_3$
OX3	-CHO	-CHO	-CHO
OX4	-CHO	-CHO	$-CH_3$

pathways resulting in a variety of products [7]. For DOPC molecules which have one double bond in each acyl chain, we considered here four representative oxidation scenarios. In two of them, we oxidized a single sn-1 acyl chain of each lipid molecule, while in the other two scenarios both sn-1 and sn-2 acyl chains were oxidized. In situ oxidation of an acyl chain was accompanied by its cleavage and termination by an aldehyde group (–CHO), accompanied by a formation of a new short chain with nine carbon atoms. In this study we considered two possible forms of this short-chain product with the cleavage site of each of the short chains being either a –CHO or a –CH group. The characteristics of the resulting four distinctly oxidized systems, denoted as OX1 to OX4, are summarized in Table 1.

MD simulations were performed using a united-atom empirical force-field for lipid molecules [8] with the parametrization for the aldehyde groups taken from Ref. [5]. The SPC model [9] was employed for water with the LINCS algorithm to constraint O–H bonds [10]. Simulations were performed for a system containing 128 lipid molecules (i.e., 64 in each leaflet of the bilayer) and 4810

water molecules in the unit cell. Periodic boundary conditions were applied with the initial size of the simulation box equal to $6.5\times6.5\times7.4$ nm^3. A non-bonded cutoff of 1 nm was employed and the Particle-Mesh-Ewald algorithm was used to account for long-range electrostatic forces [11]. The Nose-Hoover thermostat was set at 310 K and employed separately for lipids and water [12,13]. The pressure was set to 1 bar and controlled using a semi-isotropic Parrinello-Rahman pressure coupling scheme [14]. A timestep of 2 fs was employed. Before oxidation, the membrane of pure DOPC was built, equilibrated for 10 ns, and simulated for additional 100 ns. Both the area per lipid (0.68 nm^2) and electron density profiles corresponded very well with previous experimental and theoretical results [16,15]. Oxidation was performed by a cleavage of DOPC molecules based on the last snapshot of the unoxidized lipid trajectory, with the cleavage sites terminated in accord with Table 1. Each oxidized system consisted of 128 oxidized lipid molecules and either 128 (OX1, OX2) or 256 (OX3, OX4) short-chain product molecules. After oxidation, trajectories were followed for 10 ns for systems where the membrane was disintegrated, while another 10 ns was collected for systems where the membrane stability was maintained. To check longer-time behavior, the trajectory was continued for over 100 ns in the case of OX1. All calculations were performed using the GROMACS package [17].

Fig. 1 depicts final snapshots from MD trajectories of the four simulated oxidized systems. On the timescale of nanoseconds after oxidation all bilayers became destabilized and underwent structural changes. The most pronounced change was that the surface of the membrane became curved and the distances between the two leaflets increased. Also, water permeation was observed as pores formed in the membranes (Fig. 1, top views). Nevertheless,

in systems with only one of the two acyl chains of each phospholipid oxidized (OX1 and OX2) the overall integrity of the membrane was preserved during the 20 ns simulation and, as tested for OX1, was maintained even after 100 ns. In contrast, when all acyl chains were oxidized (OX3 and OX4) the bilayer disintegrated within 10 ns and micelle formation was observed. These conclusions are further supported by initial and final electron density profiles as depicted in Figure 2. As evident from this figure the basic structural properties of OX1 and OX2 system are more or less preserved along the trajectory, with the total electron density slightly decreasing with time in the headgroup regions and increasing in the membrane interior region. A qualitatively similar behavior was observed in previous simulation studies of oxidized PLPC and POPC membranes [5,6]; although, the degree of oxidation considered therein was significantly lower (up to 50%) than in the present work. Electron density profiles measured in X-ray diffraction experiments of DLPC membranes with up to 14% of oxidized lipids exhibit the same trend [18]. For the present OX1 and OX2 systems, we also observed a shift of the electron density peaks upon oxidation which corresponds to the changes of membrane thickness. In the case of OX1 the thickness decreases which is in agreement with previous calculations and was rationalized in terms of partial interdigitation of terminal methyl segments of phospholipid acyl chains [18,5]. In contrast, for OX2 the thickness increases which can be traced to the hydrophobic character of the short-chain oxidation fragments present in this system. These fragments reside into the membrane interior and they not only sterically prevent shrinking of the membrane but also hinder interdigitation of the remaining acyl chains of the phospholipid molecules. It is not yet clear why such effect was not observed for polar short-chain fragments present in the OX1 case. When all the acyl chains are oxidized (OX3 and OX4), the electron density profiles

become structureless within 10 ns, which is a clear signature of membranes disintegration.

Additional insight into structural evolution of oxidized bilayers can be obtained using distributions of tilt angles of the acyl chains and short-chain product molecules. Fig. 3 depicts for the OX1 system the distribution of tilt angles of both oxidized and unoxidized lipid chains, as well as that of the short-chain oxidation products, with respect to the normal to the bilayer. Right after oxidation all chains were oriented predominantly in parallel to the normal as in unoxidized phospholipid bilayers. As the system evolved in time, a significant fraction of oxidized chains underwent a complete orientational reversal (as also observed in a previous study [6]) but there was also a relatively large number of these chains oriented roughly parallel to the bilayer. At the same time, most of unoxidized chains preserved their original orientation and the short-chain product molecules also remained oriented mostly parallel to the membrane normal. In both fully oxidized systems (OX3 and OX4, results not depicted here) the chain reorientation was more rapid with orientation evolving towards a uniform distribution upon disintegration of the bilayer.

The area per lipid increases significantly upon oxidation for the OX1 and OX2 systems from the original value of 0.68 nm^2 pertinent for the DOPC membrane. It levels off around 0.9 and 0.78 nm^2, respectively, after about 6 ns for OX1. For comparison, in the 50% oxidized PLPC membrane the area per lipid reaches only 0.7 nm^2 [5]. In the OX3 and OX4 systems micellization occurs which effectively cancels the increase of the area per lipid. It should be noted, that for these two systems area per lipid after micellization has no longer a direct interpretation as the average area occupied by a headgroup, nevertheless, it can still be treated as a parameter that describes the structural changes in the

system. We also analyzed the kinetics of the structural changes in the oxidized membranes by monitoring the standard deviation of the position of headgroup phosphorous atoms with respect to the membrane normal. Gradual changes were observed for phospholipids with one oxidized chain (OX1 and OX2), while a runaway behavior is pertinent to the fully oxidized systems (OX3 and OX4). This is yet another indications that the OX1 and OX2 systems preserve the bilayer integrity, whereas in the OX3 and OX4 cases the membrane is destroyed at the timescale of the simulation.

One of the most interesting and practically relevant aspects of membrane oxidation is the process of pore formation. In the course of MD trajectories for both OX1 and OX2 systems formation of pores became clearly visible at around 15 ns (see Fig. 1). In the OX1 case, one or two relatively small pores formed initially, which then annihilated within tents of nanoseconds. After about 50 ns, we observed formation of larger and more stable pores, which were present for the remainder of the simulation. Fig. 4 shows in detail time evolution of such a pore displaying the cross-section of the membrane. 10 ns after oxidation the OX1 membrane structure still largely resembled that of the unoxidized lipid, although uncoupled short-chain products were present in the membrane interior. At the same time the area per lipid increased and around 40 ns headgroup interactions between leaflets occurred, accompanied by a water permeation through the membrane (Fig. 4B). Consequently, interactions between headgroups from opposite leaflets caused formation of stable hydrophilic walls of a stable pore with a diameter in the narrowest part of about 1.5 nm. Formation of such pores (Fig. 4C) is in accord with experimental findings based on neutron reflectometry for DOPC and POPC membranes under oxidative stress [19].

Based on the structural evidence described above the following mechanism of pore formation unravels. Upon oxidation a significant fraction of oxidized lipid chains tilt towards the aqueous phase, the area per lipid increases, and the lateral interactions between headgroups are weakened. Water permeation through the membrane becomes more feasible due to the increased average distance between headgroups. This permeation is accompanied by reorientation of hydrophilic headgroups which follow the water molecules. As a result, in the region of permeation a direct interaction between the headgroups located in opposite leaflets occurs, which leads to formation of stable hydrophilic walls of the pore. Also, in the final stages of pore creation the methyl groups from non-oxidized chains start to strongly interact with each other in the interior of the bilayer (see the green balls in the final snapshot in Fig. 4C).

By massively oxidizing a phospholipid membrane we were thus able to monitor formation of pores and, in certain cases, even a complete disintegration of the bilayer. Assuming an even larger degree of oxidation than pertinent to pathological conditions in living organisms we succeeded in capturing with atomistic detail the events leading to membrane disintegration using MD simulations at a computationally accessible ∼100 ns timescale. The progression and total amount of damage to the membrane depends both on the degree of oxidation and on the chemical character (hydrophobic vs amphiphilic) of the newly former short-chain fragments. When only one of the two acyl chains of each DOPC molecule is oxidized, pores form in the membrane which, nevertheless, retains its basic bilayer structure for over 100 ns. However, upon oxidation of both chains the membrane disintegrates within 10 ns, after which micellization occurs. After membrane destruction, in the system with the hydrophobic short-chain products, a hydrophobic droplet is created which is covered by

strongly oriented lipid molecules with their headgroups directed toward water phase in order to completely isolate the hydrophobic droplet from water. In the system with the amphiphilic short-chain products this droplet is also created but it is penetrated by water molecules and lipid molecules on its surface are less oriented than in the previous case.

Acknowledgments

We acknowledge support from the Czech Science Foundation via the program EUROMEMBRANES (Grant MEM/09/E006) and the Czech Ministry of Education (Grant LC512).

References

[1] H.-P. Deigner, A. Hermetter, Curr. Opin. Lipidol. 19 (2008) 289.

[2] J. Bieschke, Q. H. Zhang, E. T. Powers, R. A. Lerner, J. W. Kelly, Biochemistry 44 (2005) 4977.

[3] G. P. Gorbenko, P. K. J. Kinnunen, Chem. Phys. Lipids 141 (2006) 72.

[4] G. O. Fruhwirth, A. Loidl, A. Hermetter, Biochim. Biophys. Acta 1772 (2007) 718.

[5] J. Wong-ekkabut, Z. Xu, W. Triampo, I-M. Tang, D. P. Tieleman, Biophys J. 93 (2007) 4225.

[6] H. Khandelia, O. G. Mouritsen, Biophys. J. 96 (2009) 2734.

[7] D. A. Pratt, J. H. Mills, N. A. Porter, J. Am. Chem. Soc. 125 (2003) 5801.

[8] O. Berger, O. Edholm, F. Jahnig, Biophys. J. 72 (1997) 2002.

[9] H. J. C. Berendsen, J. P. M. Postma, W. F. van Gunsteren, J. Hermans, Interaction models for water in relation to protein hydration. In: Intermolecular Forces. Pullman, B. ed. . D. Reidel Publishing Company Dordrecht 1981 331–342.

[10] B. Hess, H. Bekker, H. J. C. Berendsen, J. G. E. M. Fraaije, J. Comput. Chem. 18 (1997) 1463.

[11] T. Darden, D. York, L. Pedersen, J. Chem. Phys. 98 (1993) 10089.

[12] S. Nose, Mol. Phys. 52 (1984) 255.

[13] W. G. Hoover, Phys. Rev. A 31 (1985) 1695.

[14] M. Parrinello, A. Rahman, J. Appl. Phys. 52 (1981) 7182.

[15] S. W. I. Siu, R. Vacha, P. Jungwirth, R. A. Bockmann, J. Chem. Phys. 128 (2008) 125103.

[16] Y. Liu, J. F. Nagle, Phys. Rev. E 69 (2004) 040901.

[17] B. Hess, C. Kutzner, D. van der Spoel, E. Lindhal, J. Chem. Theory Comput. 4, 435 (2008). GROMACS ver. 4. 0. 3, double precision compilation.

[18] R. P. Mason, M. F. Walter, P. E. Mason, Free. Radic. Biol. Med. 23 (1997) 419.

[19] H. L. Smith, M. C. Howland, A. W. Szmodis, Q. Li, L. L. Daemen, A. N. Parikh, J. Majewski, J. Am. Chem. Soc. 131 (2009) 10.

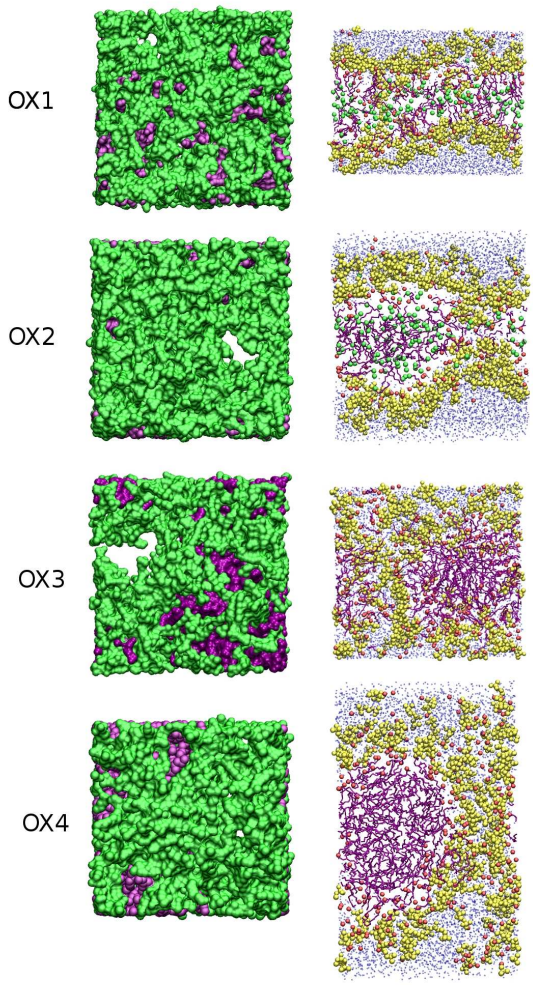

Fig. 1. Final snapshots taken for oxidized trajectories. Top- (left column) and side-view (right column) of the membranes are presented. For OX1 and OX2, which maintained their structure, the snapshots are taken 20 ns after oxidation. For OX3 and OX4, where micellization occurred, 10 ns snapshots are shown. Color coding: blue – water oxygen, green – oxidized lipid molecules, and purple – short-chain product molecules. Yellow balls depict atoms in lipid head-groups, red balls represent oxygen atoms in aldehyde groups of oxidized lipids, and green balls depict terminal methyl groups of lipid. For clarity, water molecules are omitted in the top-view snapshots. Lipid chains are omitted in side-view plots. Note the varied height of the side-view snapshots which reflects expansion of the systems upon oxidation.

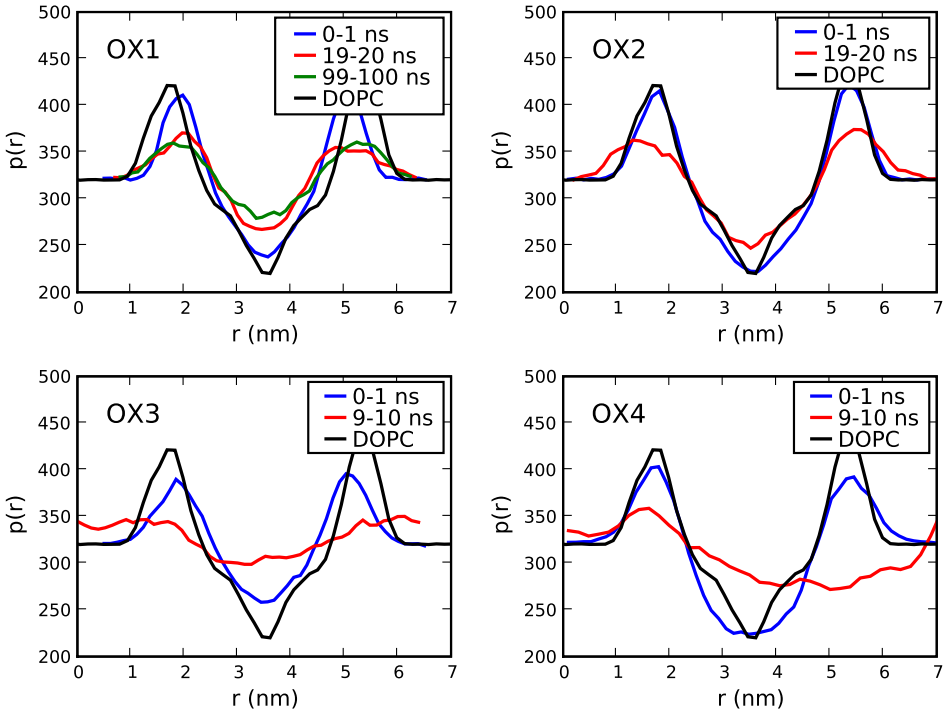

Fig. 2. Electron density profiles along a normal to the membrane calculated for one-nanosecond segments in the initial and final stages of MD trajectories upon oxidation. For OX1 the density calculated in the long-time MD run is also presented. For comparison, a pure DOPC electron density is shown in each plot.

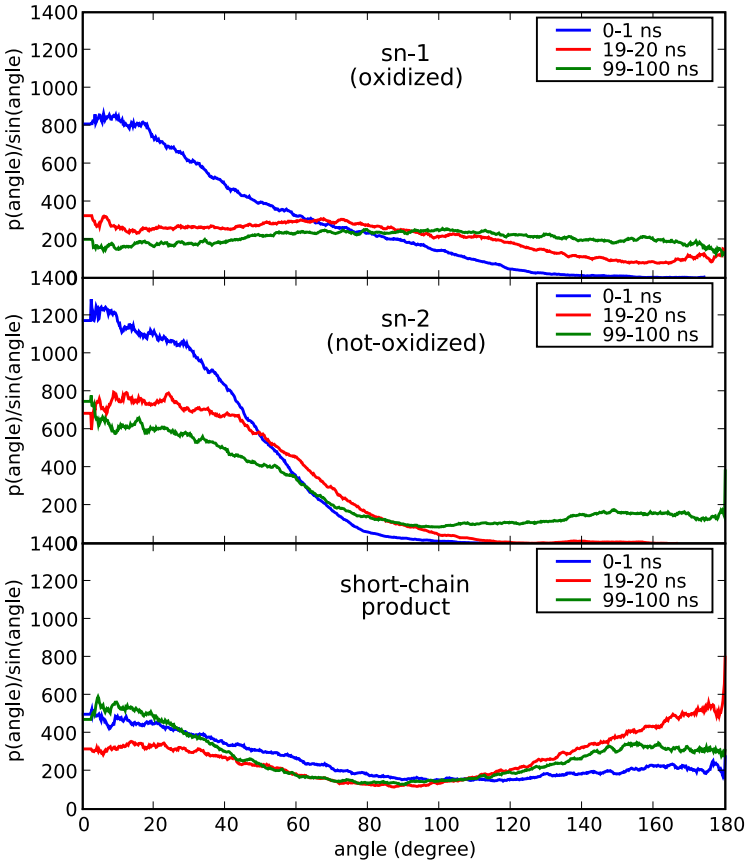

Fig. 3. Tiltangle distributions of both acyl chains of oxidized lipid and of short-chain product molecules. Data calculated at different stages of OX1 trajectory. The tiltangle is an angle between a bilayer normal and a vector connecting two terminal carbon atoms of the chain. A tilt angle of 0° indicates "unflipped" chain (for lipid chains: the terminal site directed towards membrane interior, for short-chain product: a cleavage site directed towards water phase), a tiltangle of 180°corresponds to a "flipped" chain.

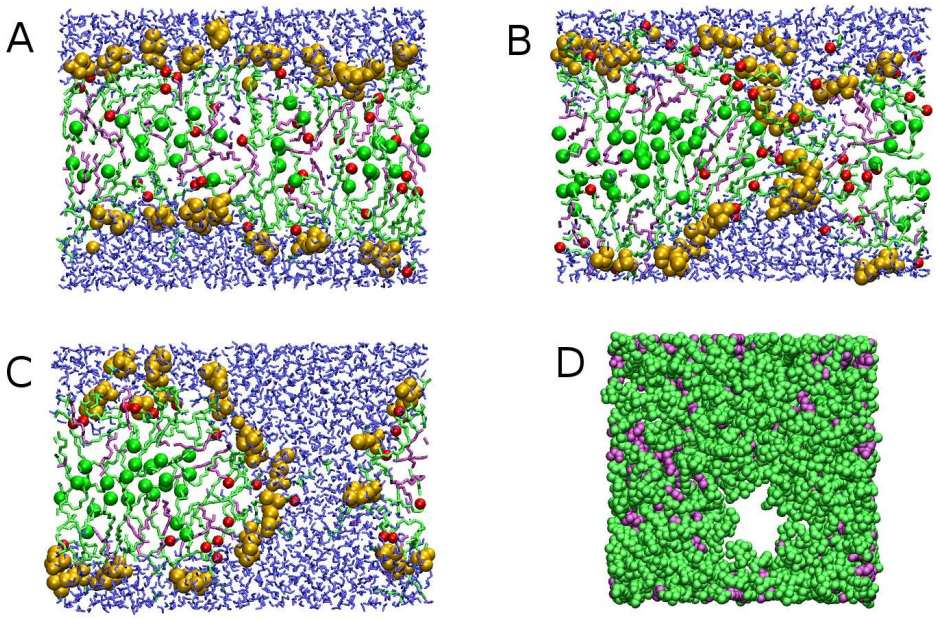

Fig. 4. Formation of a pore in OX1 trajectory. Side-view cross-sections made at the center of the pore using snapshots taken at 10, 40 and 110 ns are presented in (A), (B) and (C), respectively. Plot (D) depicts the top view of the system at 110 ns upon oxidation, note the pore visible as the white region. The color coding is as in Fig. 1. Lipid chains, omitted in Fig. 1, are shown here as green licorices. For clarity, only the molecules belonging to the nearest neighborhood of the pore are depicted.